Hindawi
Journal of Mathematics
Volume 2023, Article ID 3763147, 12 pages
https://doi.org/10.1155/2023/3763147

Research Article

Numerical Investigation of the Finite Thin Film Flow for Hybrid Nanofluid with Kerosene Oil as Base Fluid over a Stretching Surface along with the Viscous Dissipation and Variable Thermal Conductivity Effects

Yasir Mehmood,[1] **Ammar Alsinai**,[2] **Ramsha Shafqat**,[1] **Muhammad Bilal**,[3] **Allah Yar Khan**,[1] **and Read S. A. Qahtan**[4]

[1]*Department of Mathematics and Statistics, The University of Lahore, Sargodha 40100, Pakistan*
[2]*Department of Mathematics, Kuvempu University, Shivamogga, Karnataka 577451, India*
[3]*Department of Mathematics, The University of Chenab, Gujrat, Pakistan*
[4]*Department of Mathematics, Aljanad University for Science and Technology, Taiz, Yemen*

Correspondence should be addressed to Read S. A. Qahtan; readsaleh2015@gmail.com

Received 8 February 2023; Revised 29 March 2023; Accepted 2 November 2023; Published 16 November 2023

Academic Editor: Qingkai Zhao

This study examines the flow and heat transfer of a finite thin layer of a hybrid nanofluid across an unstable stretching surface with varying thermal conductivity and viscous dissipation effects. A hybrid nanofluid model is considered to comprise two different types of nanoparticles, Go and Ag, with kerosene oil used as a base fluid. To study the phenomenon of thermal conduction, a modified version of Fourier's law model is adopted because in the power-law model, the thermal conductivity depends on the velocity gradient. A system of nonlinear ordinary differential equations is obtained by considering the similarity transformations over the obtained rheological system of partial differential equations which is then tackled by a well-known numerical approach, i.e., the bvp4c MATLAB technique. The rheological impacts of the power-law index, solid volume fraction, film thickness, Eckert number, and modified Prandtl number on temperature and velocity fields are graphically discussed and illustrated. In the presence of nanoparticles, the temperature of the working fluid is enhanced and the power-law index has an inverse relation with the velocity of the hybrid nanofluid.

1. Introduction

Thin film is a layer of material ranging from a fraction of nanometer (10^{-9}) to several micrometer (10^{-6}) in thickness. The thin film flow analysis is very valuable due to its inclusive applications in the engineering and technology field. The thin film flow problems have a broader area of interest and catch many fields, starting from flow inside the human lungs to industrial coating problems. It is much important to explore the thin film flow uses in structural mechanics, theology, and fluid mechanics. The liquid film has well-known uses such as the expulsion of polymer and metal, constant forming, foodstuff processing, drawing elastic sheets and devices, fluidization, and exchanges. For inspection of these uses and applications, the researchers are motivated to further investigate and make further development in the field of thin-film flow problems. Different approaches are adopted with modified geometries. In industrial applications, the stretching surface is a major topic. Gul et al. [1] worked on the flow of third-grade magnetohydrodynamic (MHD) fluid with an impact on viscosity (temperature dependent) on a vertical belt. Later on, Bachicha [2] explored a method for producing cathodes from thin-filmed coatings which are produced by placing

catholyte slime on a moving substrate. Aqil et al. [3] found that when the pure molybdenum (Mo) thin film (by the DC magnetron sputtering technique) is deposited on the blank Si substrate, the deposition condition only changed for the deposition time, not for all other samples. Afterwards, Shah et al. [4] examined the effect of thermal radiations on a permeable medium and heat generation through a stretching surface during the Williamson liquid-film fluid flow. They considered the fluid flow in two dimensions of liquid films. Ullah et al. [5] worked on the flow (with skid conditions) of a generalized Maxwell fluid that is flowing on a nonisothermal cylindrical surface.

Heat generation plays an important role in the flow of a thin film. When any type of energy inside the body is transferred into heat energy, then the temperature of the body increases which causes heat generation. The body is made up of atoms and molecules, and when any type of energy is applied to the body, the atoms and molecules start vibrating, which makes friction; as a result, heat is generated. In industries and engineering, the transfer of heat over the moving continuous stretching sheet is investigated frequently due to its many applications. To set the standard of any product in the industry, heat generation plays an important role. Heat generation is majorly affected by temperature diffusion and the particle toppling rate in a chemical reaction. Chankha and Issa [6] worked on the impact of heat generation and thermogenesis in hydromagnetics with mass and heat transfer through a permeable flat surface. Afterwards, the impact of heat generation, as well as radiation due to the linearly stretching sheet through an incompressible micropolar fluid, is highlighted by Reddy [7]. Mehmood et al. [8] worked on the numerical investigation of MWCNT and SWCNT fluid flow along with the activation energy effects over quartic autocatalytic endothermic and exothermic chemical reactions. Pavithra and Gireesha [9] numerically examined a boundary flow and heat transfer for the dusty fluid in the existence of internal heat generation and viscous dissipation over an explosive/accelerating stretching surface. Later on, a comprehensive review of heat generation in various types of wastes was taken by Yeşiller et al. [10]. Ganga et al. [11] illustrated the heat generation on the boundary layer magnetohydrodynamic flow of nanofluids. The heat generation effects over the stretching surface in the flow of non-Newtonian nanofluid are explored by Awais et al. [12]. Aziz et al. [13] studied the impact of heat generation on magnetonanofluid. Later on, the influence of heat generation over MHD Oldroyd B fluid with radiation on an inclined stretching sheet is examined by Mabood et al. [14]. Khan et al. [15] explored the heat generation impact on the heated surface during the chemically reactive flow. Nanofluid is a fluid having nanometer-size (10^{-9}) particles, called nanoparticles. The nanoparticles are naturally made of metals, fibers, tubes, wires, rods, sheets, droplets, oxides, or carbon nanotubes. Nanofluids are mostly used to improve the thermophysical properties such as viscosity, thermal conductivity, thermal diffusivity, and heat transfer (depending on thermal conductivity) coefficients to differentiate base fluids (water or oil). They are very valuable for the cooling of a microsystem. It has many applications in many fields. Fluids such as water, oil, and ethylene glycol in these processes have been considered as cooling liquids but have a limited heat transfer rate. Wong and De Leon [16] focused on the broader scope of heat and the applications that demand nanofluids. A review (theoretical and experimental) of nanofluid for the magnification of thermal conductivity is studied by Kleinstreuer and Feng [17]. Fluids in which two or more nanometer-size particles of different materials are mixed into the base fluid to get the desired physical properties are called hybrid nanofluids. These are being used to further enhance the heat transfer rate, pressure drop properties, better thermal network, and collaborative effect of nanomaterials. In the case of nanofluids, we have to face some major issues. One of them considered the stability of nanofluids, and it has become a big challenge to attain the required characteristics. The properties of hybrid nanofluids are investigated by researchers to find out their applications, advantages, and disadvantages. Madhesh and Kalaiselvan [18] experimentally used the tubular heat exchanger to study the heat transfer through a hybrid nanofluid. In their work, they explored the effects of the thermal characteristics and also analyzed the hybrid nanofluids as coolants. Later on, Hayat and Nadeem [19] explained the use of Ag + CuO as a hybrid nanofluid to improve the heat transfer rate. Afterwards, Sundar et al. [20] took a review for the friction factor, heat transfer, and thermal properties of hybrid nanofluid. Similarly, Minea and Moldoveanu [21] worked on the development and benefits of hybrid nanofluids. The steady, laminar, incompressible two-dimensional flow over the static channel using hybrid nanofluid (TiO_2+ CuO/water) is examined by Dinarvand et al. [22]. A mass-based approach has been presented for the hybrid nanofluid model. Bumataria et al. [23] analyzed the rate of heat transfer through a pipe and discussed it with applications for hybrid nanofluids. Some recent work related to nanofluid and hybrid nanofluid can be cited in [24–26].

When any shear force is applied to the fluid, then this force passes through the adjacent layers and hence the work done because of this force is transferred into heat; this process is called viscous dissipation. High rotational speed devices which have a strong impact on the gravitational field also have an essential part of viscous dissipation for their natural convection. Viscous dissipation also has an important part in geographical and nuclear physics. Many researchers have identified viscous dissipation by using nondimensional Eckert numbers. In gravitational fields, such as large planets, the remarkable effects of viscous dissipation may also exist. Massoudi and Christie [27] worked on the thermodynamically frictionless, incompressible third-grade fluid flow to investigate the reaction of viscosity (variable) and viscous dissipation. Later on, Mehmood et al. [28] numerically examined the boundary layer nanofluid flow due to mass flux conditions and viscous dissipation in a bent stretching surface. Pandey and Kumar [29] explored the MHD nanofluid flow, with injection and viscous dissipation over the porous medium and slip flow. Afterwards, Ahmed et al. [30] studied a nanofluid flow with the additional impact of viscous

dissipation. The KKL model is implemented for the thermal conductivity of nanofluids and the solid nanoparticles of copper oxide. Mishra and Kumar [31] explored the effects of heat absorption on nanofluid (Ag) in the existence of suction/injection through a vertical Riga plate. Using the homotopy perturbation technique, the fluid flow due to viscous dissipation and variable temperature-dependent conductivity along with magnetohydrodynamic over a flat plate is studied by Saxena [32]. Masood et al. [33] worked on the MHD flow of a nanofluid in the biomedical field to describe the viscous dissipation impact on velocity and temperature properties.

Pseudoplastic fluids are a type of non-Newtonian fluid. These are shear-thinning fluids because viscosity decreases in these fluids. Viscosity decreases when shear forces are increased. Because of their many applications in industry, these fluids have much importance. Guedda and Kersner [34] studied the exact and analytical results of non-Newtonian pseudoplastic (Cu, Al_2O_3, and TiO_2) fluids. Afterwards, Ma et al. [35] examined the turbulent and laminar pseudoplastic fluid flow containing CMC-water through a square duct by using microphones and ultrasonic Doppler velocity. The fluctuating pressure and duct velocity for different flow rates were measured. Das et al. [36] worked on entropy analysis with heat convection by using a porous channel of pseudoplastic MHD nanofluid flow. Ayoubi Ayoubloo at el. [37] used a porous layer on a cylindrical cavity (vertical, partially filled) to investigate the heat transfer and natural convection flow behavior of the pseudoplastic fluid.

The main objective of the present study is to discuss the numerical investigation of finite thin-film flow for hybrid nanofluid with kerosene oil as base fluid over a stretching surface. In it, we have considered graphene oxide and silver as the nanoparticles. Kerosene oil (K) with a graphene oxide (GO) basis may be able to aid in parabolic trough surface accumulator (PTSC) performance monitoring. The heat transition rate of GO-K is 15.03% greater than that of regular fluid devoid of GO. Theoretical simulations supported by documentation may be more beneficial for enhancing solar thermal energy plans. Applications for a PTSC include heating homes, distillation, cooling systems, manufacturing heat, power plants, and irrigation water pumps. A modified Fourier's law is adopted to discuss the phenomenon of pseudoplastic fluid. Instead of using a simple fluid or nanofluid specifically in this article, we have considered hybrid nanofluids and the influence of internal viscous dissipation is also taken into account. As far as we are aware, no such study has been carried out. The bvp4c MATLAB function is employed to solve the governing problem numerically. The effects on temperature and velocity field for the viscous dissipation, power-law index, thickness parameter, unsteadiness parameter, and Prandtl number are studied and graphically shown.

2. Mathematical Model

Presume a parallel stretching surface with a small gap through which a pseudoplastic hybrid nanofluid is flowing in a thin finite layer under shear-thinning conditions. Figure 1 depicts a schematic physical model and coordinate system. The fluid is made to move as a rapid response to the sheet that is stretching along the x-axis. The sheet at $y = 0$ is riveted with the x-axis which has the temperature distribution $T_w(x,t)$ and moves with velocity $u_w(x,t)$. A thin film reclines on a stretching surface with thickness $h(x,t)$. Hybrid nanofluid is considered which is incompressible, and thermal equilibrium holds for both base fluid and hybrid nanoparticles. It is also presumed that the viscous dissipation phenomenon is also contained in the stretching sheet. The sheet is stretched, giving the liquid film a flat surface and preventing the production of waves. The heat flow and viscous shear stress are eliminated by this adiabatic-free surface. Furthermore, the flow is considered laminar, incompressible, and irrotational. Thermophysical properties of the base fluid and nanoparticles (graphene oxide and silver) are given in Table 1. According to all these premises, governing equations for momentum and energy can be written as follows [38, 39]:

$$\frac{\partial v}{\partial y} + \frac{\partial u}{\partial x} = 0, \tag{1}$$

$$u\frac{\partial u}{\partial x} + \frac{\partial u}{\partial t} + v\frac{\partial u}{\partial y} = \frac{\partial}{\partial x}\left(\frac{\mu_{\text{hnf}}}{\rho_{\text{hnf}}}\frac{\partial u}{\partial y}\left|\frac{\partial u}{\partial y}\right|^{n-1}\right), \tag{2}$$

$$u\frac{\partial T}{\partial x} + \frac{\partial T}{\partial t} + v\frac{\partial T}{\partial y} = \frac{\partial}{\partial y}\left(\alpha_{\text{hnf}}\frac{\partial T}{\partial y}\left|\frac{\partial u}{\partial y}\right|^{n-1}\right) + \frac{\mu_{\text{hnf}}}{\left(\rho C_p\right)_{\text{hnf}}}\left|\frac{\partial u}{\partial y}\right|^{n-1}\left(\frac{\partial u}{\partial y}\right)^2. \tag{3}$$

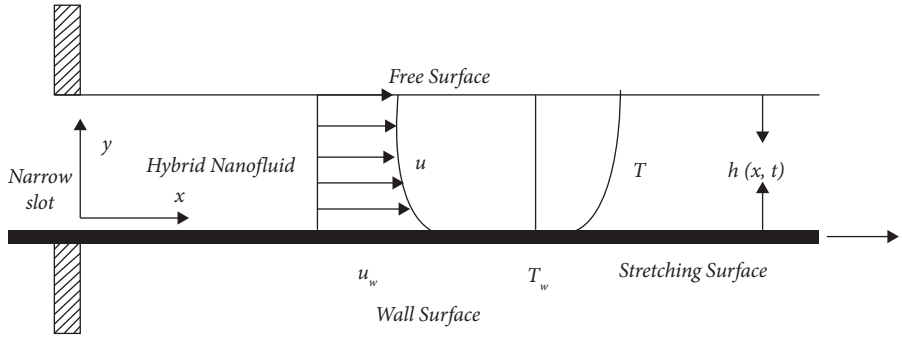

Figure 1: Geometry of the model.

Table 1: Thermophysical properties of base fluid and nanoparticles.

Physical properties	GO	Ag	Kerosene oil
ρ (kg.m^{-3})	1800	10500	783
C_p (J(kg.°k))	717	235	2090
σ (Ω.m)	6.30×10^7	63×10^{-6}	21×10^{-6}
k (W(m.°k)	5000	429	0.145

The coefficients $\mu_{\text{hnf}}/\rho_{\text{hnf}}|\partial u/\partial y|^{n-1}$ from equation (2), and $\alpha_{\text{hnf}}|\partial u/\partial y|^{n-1}$ and $\mu_{\text{hnf}}/(\rho C_p)_{\text{hnf}}|\partial u/\partial y|^{n-1}$ from equation (3) represent the property of the pseudoplastic fluid. Following are the boundary conditions [39]:

$$\left.\begin{aligned} &y = 0, \quad v = 0, \quad T = T_w, u = u_w \\ &y \longrightarrow h(x,t), \frac{\partial T}{\partial y} = \frac{\partial u}{\partial y} = 0, \quad v = \frac{\partial h}{\partial t} + u\frac{\partial h}{\partial x} \end{aligned}\right\}, \tag{4}$$

where u and v represents the components of velocity along the x and y axes, respectively, t shows time, $\tau_{xy} = \mu_{\text{hnf}}|\partial u/\partial y|^{n-1}\partial u/\partial y$ is the shear stress, $\mu = \mu_{\text{hnf}}|\partial u/\partial y|^{n-1}$ is the nanofluid effective viscosity, μ_{hnf} is the coefficient of modified consistency viscosity, ρ_{hnf} shows the nanofluid effective density, and n shows the power-law index. In the case of Newtonian fluid $n = 1$, for pseudoplastic fluid, $0 < n < 1$, while $n > 1$ describes a dilatant fluid. T shows temperature, C_p and ρC_p are the specific heat and effective heat capacities, respectively, and $h(x,t)$ is the nanofluid film thickness. For the fluid motion, a kinematics constraint is imposed by $v = u\partial h/\partial x + \partial h/\partial x$. The power-law viscosity effects are considered on the temperature field by assuming that temperature and velocity fields are similar and thermal conductivity is dependent on velocity, for example, $k = \alpha_{\text{hnf}}(\rho C_p)_{\text{hnf}}|\partial u/\partial y|^{n-1}$ and $\alpha_{\text{hnf}}|\partial u/\partial y|^{n-1}$ shows the effective thermal diffusivity. The effect of velocity dissipation is composed by the term $\mu_{\text{hnf}}/(\rho C_p)_{\text{hnf}}|\partial u/\partial y|^{n-1}(\partial u/\partial y)^2$.

When the wall surface is stretched at $y = 0$, this causes a flow such that the sheet moves with velocity u_w along x-direction as

$$u_w = \frac{bx}{(1-at)}, \tag{5}$$

where both a and b are constants having a positive value with $(\text{sec})^{-1}$ dimensions. The temperature T_w of wall surface differ with slot distance x and time t as

$$T_w = T_o - T_{\text{ref}} b^{2-n} x^2 (1-at)^{-2}\gamma^{-1}, \tag{6}$$

where $\gamma_f = \mu_f/\rho_f$ shows modified kinematic viscosity and μ_f shows modified viscosity for base fluid, T_o is the origin temperature, ρ_f is the base fluid density, and T_{ref} shows reference temperature that may be considered as the constant. The values of u_w and T_w from equations (5) and (6), respectively, help us to develop a transformation that converts governing PDEs into ODEs. Moreover, μ_{hnf} is considered as the hybrid nanofluid fluid viscosity and dilute suspension is contained by μ_f and is defined by Brinkman as

$$\mu_{\text{hnf}} = \frac{\mu_f}{(1-\phi_1)^{2.5}(1-\phi_2)^{2.5}}, \tag{7}$$

where ϕ stands for the solid volume fraction of nanoliquid. To properly define the stream function, such as $u = \partial\psi/\partial y$ and $v = -\partial\psi/\partial x$, some important transformation variables are used as follows:

$$\begin{aligned}\psi(x,y,t) &= b^{(2n-1)/(n+1)}\gamma_f^{1/(n+1)}x^{2n/(n+1)}(1-at)^{(1-2n)/(n+1)}f(\eta),\\ \eta &= b^{(2-n)/(n+1)}\gamma^{-1/(n+1)}x^{(1-n)/(n+1)}(1-at)^{(1-2n)/(n+1)}y,\\ T &= T_o - T_{\text{ref}}b^{(2-n)}x^2\gamma^{-1}(1-at)^{-2}\theta(\eta),\\ \beta &= b^{(2-n)/(n+1)}\gamma^{-1\,1/(1-n)}x^{(1-n)/(n+1)}(1-at)^{(n-2)/(n+1)}h(x,t).\end{aligned} \tag{8}$$

The nondimensional parameters which are used for the conversion purpose are as follows:

$$\begin{aligned}\text{Re}_x &= \frac{u_w^{2-n}x^n}{\gamma_f} = \frac{b^{2-n}x^2}{\gamma_f}(1-at)^{n-2},\\ \text{Pr} &= \frac{\mu_f}{\rho_f} = \frac{(\rho C_p)_f}{k_n} = \gamma_f\frac{(\rho C_p)_f}{k_n},\\ S &= \frac{a}{b},\\ \text{Ec} &= \frac{\mu_f}{(\rho C_p)_f}\frac{b^n}{T_{\text{ref}}},\end{aligned} \tag{9}$$

where β is the nanoliquid film thickness, Re_x shows the local Reynolds number, Pr shows Prandtl number, S represents the unsteadiness parameter, and Ec shows the Eckert number. The rest of the physical properties of nanofluid are defined as

$$\begin{aligned}\rho_{\text{hnf}} &= \rho_f\left[(1-\phi_1)+\frac{\rho_{s1}}{\rho_f}\phi_1\right](1-\phi_2)+\phi_2\rho_{s2},\\ (\rho C_p)_{\text{hnf}} &= \left[(1-\phi_1)+\frac{(\rho C_p)_{s1}}{(\rho C_p)_f}\phi_1\right](1-\phi_2)(\rho C_p)_f+\phi_2(\rho C_p)_{s2},\\ k_{\text{hnf}} &= \frac{(k_{s2}+2k_{nf})-2\phi_2(k_{s2}-k_{nf})}{(k_{s2}+2k_{nf})+\phi_2(k_{s2}-k_{nf})}\times k_{nf},\end{aligned} \tag{10}$$

where ρ_{s1},ρ_{s2} and $(\rho C_p)_{s1},(\rho C_p)_{s2}$ represent the solid density and solid heat capacity, respectively, $(\rho C_p)_f$ stands for the base fluid heat capacity, k_{nf} and k_f show modified thermal conductivity and thermal conductivity of base fluid, while k_s is the thermal conductivity of solid particles. All abovementioned nondimensional parameters and dimensionless transformations are used for individualized growing of PDEs. The value of velocity components u and v are given as

$$\begin{aligned}u &= \frac{bx}{(1-at)}f'(\eta),\\ v &= -Re_x^{-1/(n+1)}u_w\left[\frac{2n}{(n+1)}f(\eta)-\frac{(n-1)}{(n+1)}\eta f'(\eta)\right].\end{aligned} \tag{11}$$

After simplification, we convert them into the following ODEs:

$$\begin{aligned}&\left(\left|f''\right|^{n-1}f''\right)' - \frac{A_2}{A_1}\left[S\left(f'+\frac{2-n}{n+1}\eta f''\right)+f'^2-\frac{2n}{n+1}ff''\right]=0,\\ &\left(\left|f''\right|^{n-1}\theta'\right)' - \frac{A_3\text{Pr}}{A_4}\left[Ec\left|f''\right|^{n+1}+\frac{A_1}{A_3}\left[S\left(2\theta+\frac{2-n}{n+1}\eta\theta'\right)+\left(2f'\theta-\frac{2n}{n+1}f\theta'\right)\right]\right]=0.\end{aligned} \tag{12}$$

The boundary conditions are

$$
\begin{aligned}
f(0) &= 0,\\
f'(0) &= 1,\\
\theta(0) &= 1,\\
f(\beta) &= \frac{2-n}{2n}\beta S,\\
f''(\beta) &= 0,\\
\theta'(\beta) &= 0.
\end{aligned}
\tag{13}
$$

3. Numerical Solution

The higher-order ordinary differential equations are transformed into the system of 1st order ODEs by using f, f', f'', θ, and θ' as y_1, y_2, y_3, y_4, and y_5 with six reformed boundary conditions. The parameters β and S are the two key features that represent the thickness and unsteadiness, respectively, and also have a dependence relation. Due to this relation, six boundary conditions are reduced into five. This reformed system is numerically solved by using the MATLAB built-in function bvp4c. Let the convective notations which are used with their boundary conditions are

$$
\left.
\begin{aligned}
y_2 &= y_1', && 0 = y_1(0)\\
y_3 &= y_2', && 1 = y_2(0)\\
\frac{A_2}{A_1}\frac{(y_3)^{1-n}}{n}\left[S\left(y_2 + \frac{2-n}{n+1}\eta y_3\right) + y_2^2 - \frac{2n}{n+1}y_1 y_3\right] &= y_3', && 0 = y_3(\beta)\\
y_5 &= y_4', && 1 = y_4(0)\\
y_3^{1-n}\frac{A_3\mathrm{Pr}}{A_4}\left\{\frac{A_1}{A_3}\left[Ec|y_3|^{n+1} + S\left(2y_4 + \frac{2-n}{n+1}\eta y_5\right) + 2y_2 y_4 - \frac{2n}{n+1}y_1 y_5\right]\right.&\\
\left. + (n-1)y_5|y_3|^{n-2}y_3'\right\} &= y_5', && 0 = y_5(\beta)
\end{aligned}
\right\},
\tag{14}
$$

$$
\begin{aligned}
A_1 &= \frac{1}{(1-\phi_1)^{2.5}(1-\phi_2)^{2.5}},\\
A_2 &= \left[(1-\phi_1) + \frac{\rho_1}{\rho_f}\phi_1\right](1-\phi_2) + \phi_2\frac{\rho_2}{\rho_f},\\
A_3 &= \left[(1-\phi_1) + \frac{(\rho C_p)_{s1}}{(\rho C_p)_f}\phi_1\right](1-\phi_2)(\rho C_p)_f + \phi_2(\rho C_p)_{s2},\\
A_4 &= \frac{(k_{s2}+2k_{nf}) + 2\phi_2(k_{s2}-k_{nf})}{(k_{s2}+2k_{nf}) - \phi_2(k_{s2}-k_{nf})}\left(\frac{(k_s+2k_f) - 2\phi_1(k_f-k_s)}{(k_s+2k_f) + \phi_1(k_f-k_s)}\right).
\end{aligned}
$$

Table 2 displays a role of comparison of the numerical results which are considered for the limiting case. The obtained results are quite evident that these are aligned with the previous work in true spirit.

4. Results and Discussion

MATLAB is used to obtain the solution using bvp4c. The toleration is maintained at 10^{-5}. The behavior of velocity and temperature profiles has been inspected by varying the numeric values of distinguished parameters. The kerosene oil as base fluid is taken with GO + Ag as a hybrid nanoparticle. The overall working of the model is shown in Figure 2, in which the whole model is divided into three main steps. The rheological values of $-\theta'(0)$ are given for different parameters mentioned in Table 3.

Figures 3 and 4 illustrate the impact of n, which ultimately affects $f'(\eta)$ (velocity) and $\theta(\eta)$ (temperature) of hybrid nanofluid, while all the other physical parameters are fixed, i.e., $\phi_1 = 3\%$, $\phi_2 = 5\%$, $\mathrm{Pr} = 0.76$, $\mathrm{Ec} = 0.01$, and $S = 1$.

Table 2: Comparison of current numerical outcomes with the earlier work in the limiting case.

		$-f''(0)$		
Parameters		Comparison analysis		
S	β	Wang and Pop [40]	Lin et al. [38]	Current
0.8	2.152	1.24580	1.2457	1.2457
1	1.543	1.27777	1.2777	1.2777
1.2	1.128	1.27918	1.2790	1.2790

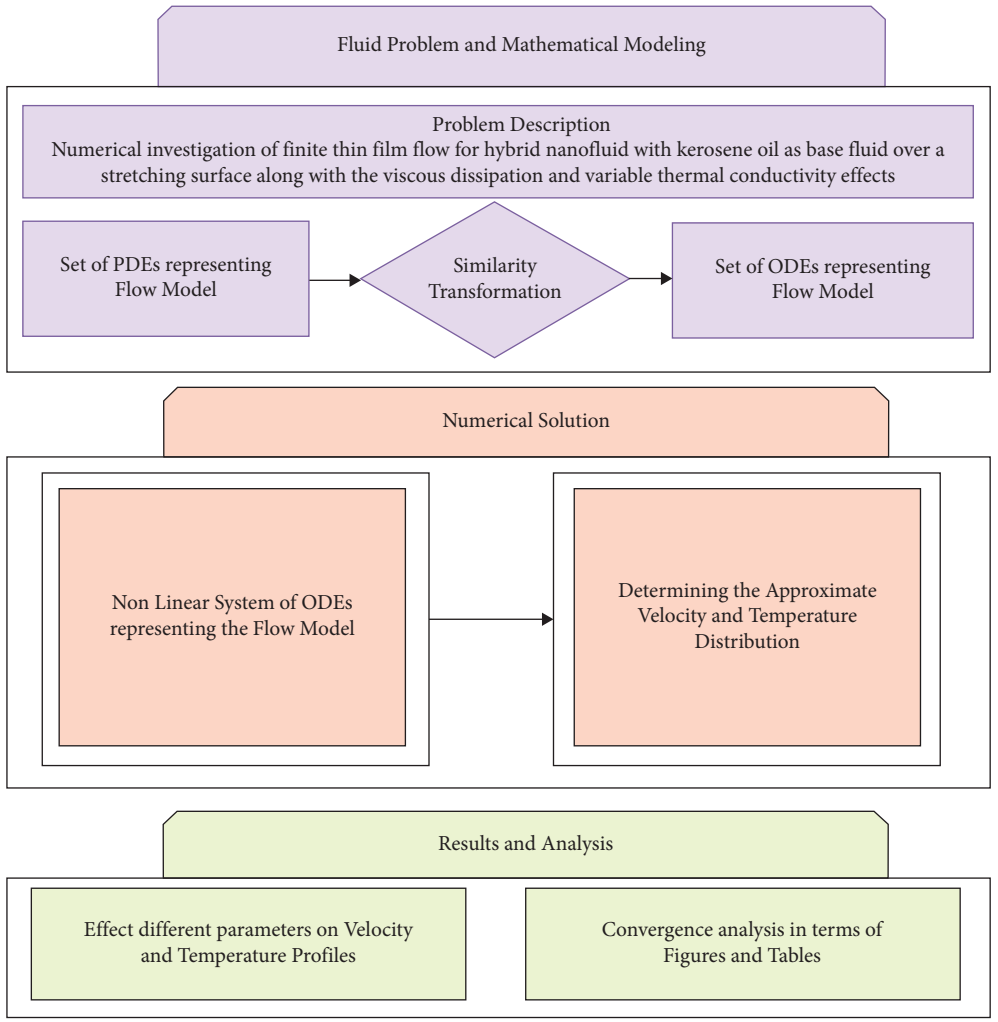

Figure 2: Working flowchart.

Table 3: Numerical results of the Nusselt number for different parameters.

n	S	β	Pr	Ec	ϕ_1	$-\theta'(0)$
0.78	1.0	0.6160	0.7	0.1	0.02	1.12461466
0.83		0.7936				1.19979379
0.93		0.9320				1.19979379
	1.2					1.17867313
	1.4					1.31373862
	1.6					1.50006595
			1			1.84258519
			1.3			2.16182090
			1.6			2.44031664
				0.5		1.54309820

Table 3: Continued.

n	S	β	Pr	Ec	ϕ_1	$-\theta^{'}(0)$
				1		1.64463687
				1.5		1.74617555
					0.04	1.45236670
					0.06	1.44272534
					0.08	1.43292776

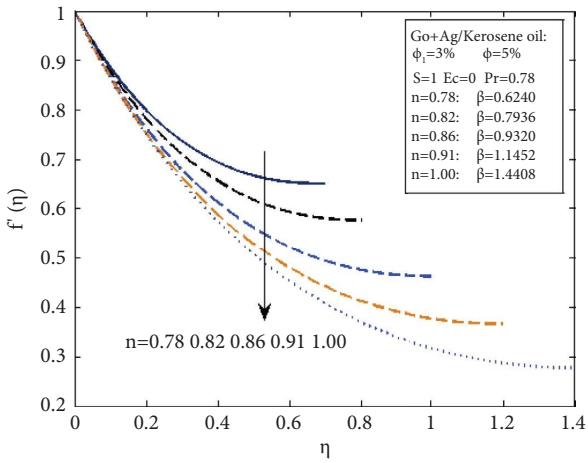

Figure 3: Impact of n on $f^{'}(\eta)$ (velocity).

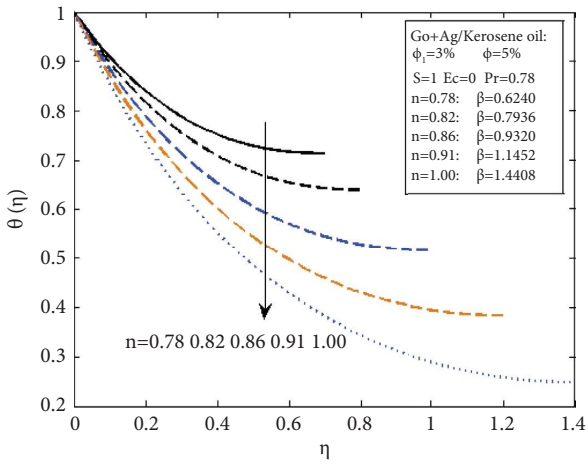

Figure 4: Impact of n on $\theta(\eta)$ (temperature).

The value of $f^{'}(\eta)$ (velocity) is turned down due to an expansion in the power-law index n. So, upon higher values of n, the velocity of the hybrid nanofluid becomes lower. As we know that for $n = 1$, we have a Newtonian fluid, shear thickening fluid for $n > 1$, and for $n < 1$, we have shear-thinning fluid. While enhancing the power-law index, the shear thickening impact is produced that happens due to higher viscosity and ultimately reduces the working fluid's velocity. For the larger n, speed goes down, so ultimately, the kinetic energy of the molecules gets slower and resultantly shows a decrement in the temperature. So, they also have an inverse relation.

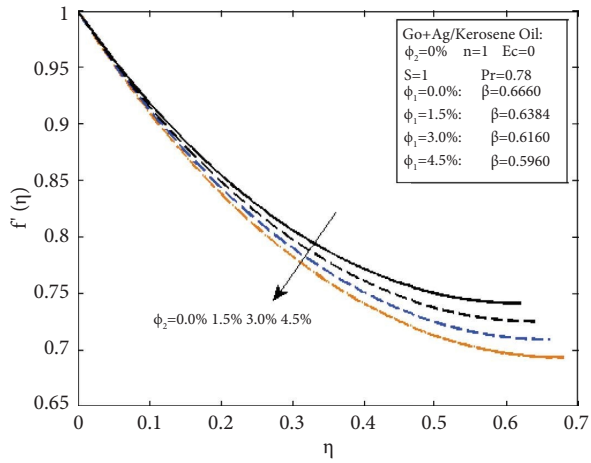

Figure 5: Impact of ϕ_1 on $f^{'}(\eta)$ (velocity).

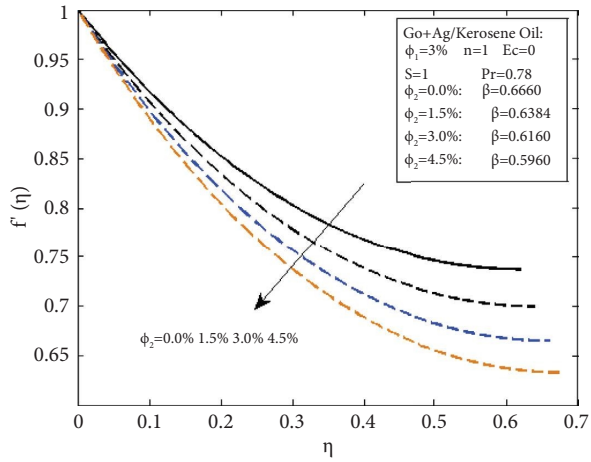

Figure 6: Impact of ϕ_2 on $f^{'}(\eta)$ (velocity).

Figures 5 and 6 represent the relationship between ϕ (solid volume fraction) and $f^{'}(\eta)$ (velocity) and $\theta(\eta)$ (temperature), respectively. For hybrid nanofluids, solid volume fraction contains two different types of nanoparticles; first, ϕ_1 is treated as a variable, i.e., $\phi_1 = (0\%, 1.5\%, 3\%, 4.5\%,)$ while ϕ_2 is considered fix. Here, it is important to note that ϕ_1 denotes the volume fraction of graphene oxide and ϕ_2 of silver. As the numeric values of ϕ_1 lead to a rise, the velocity profile moves up. The difference in velocity between the wall and free surface is striking due to the exploits of ϕ_1. A similar impact on the velocity profile is eminent for ϕ_2 of the second type of nanoparticles. Again, the velocity rises for the higher values of ϕ_2.

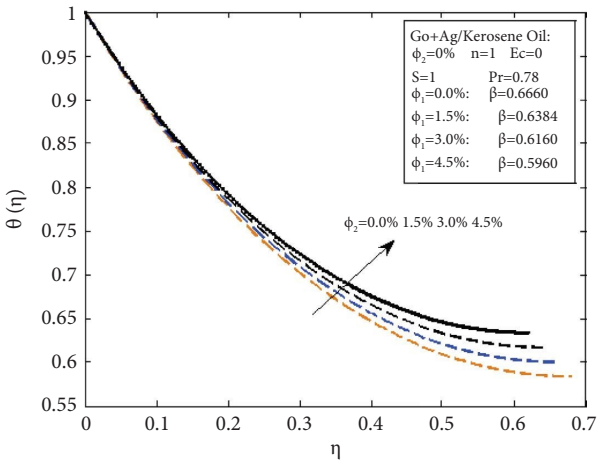

Figure 7: Impact of ϕ_1 on $\theta(\eta)$ (temperature).

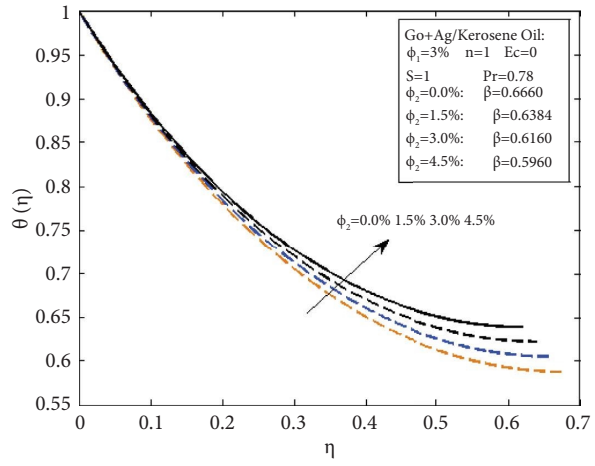

Figure 8: Impact of ϕ_2 on $\theta(\eta)$ (temperature).

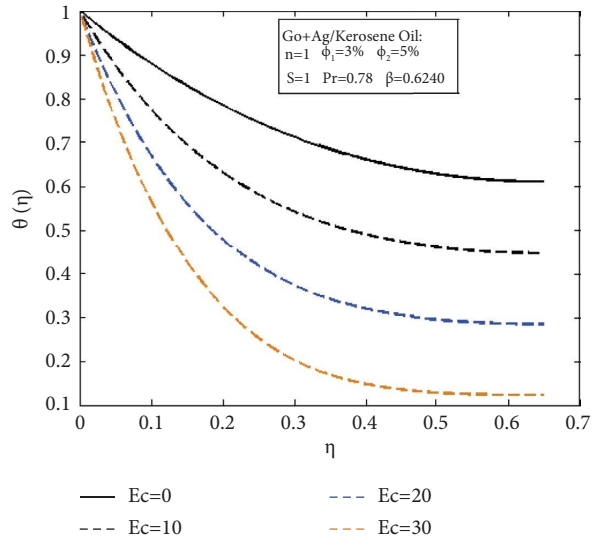

Figure 9: Impact of Ec on $\theta(\eta)$.

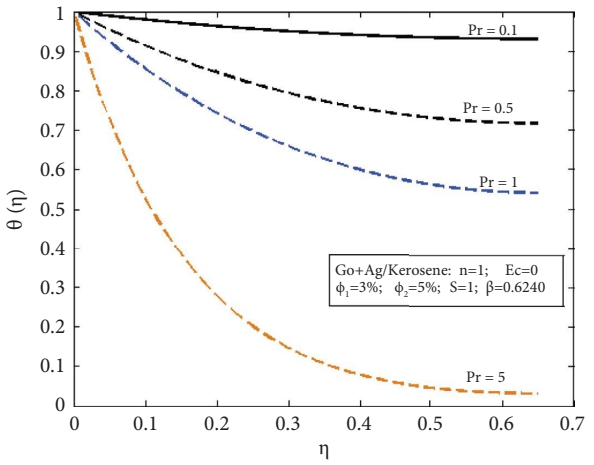

Figure 10: Impact of Pr on $\theta(\eta)$.

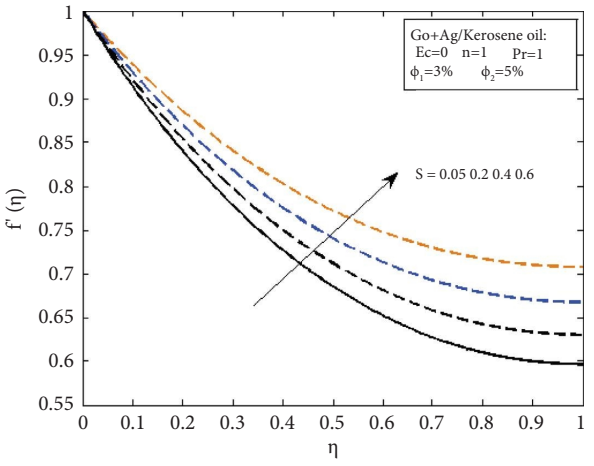

Figure 11: Impact of S on $f'(\eta)$ (velocity).

The relation between ϕ (solid volume fraction) and $\theta(\eta)$ (temperature) is perceived in Figures 7 and 8 by presuming two cases regarding nanoparticles ϕ_1 and ϕ_2. In Figure 7, ϕ_1 grips as a variable, i.e., $\phi_1 = (0.0\%, 1.5\%, 3\%, 4.5\%)$, while ϕ_2 that shows the volume fraction of silver and all the other parameters are taken constantly. It is noted that as the ϕ_1 elevated, the temperature escalates. Due to the presence of hybrid fluid, the thermal conductivity enhances and the increment in thermal conductivity increases the temperature. The consequences are almost similar to the previous case when ϕ_2 is considered a variable, while ϕ_1 and all other parameters are considered constant. So, there is a direct relation between ϕ and $\theta(\eta)$, i.e., as the film solid volume portion rises so does its temperature.

Figure 9 describes the effects on $\theta(\eta)$ (temperature) due to the presence of viscous dissipation (Eckert number) Ec with hybrid nanofluid. The results demonstrate that the heat transfer process is dependent on the Eckert number. It is observed that when the value of the Eckert number grows

(Ec = 0, 2, 4, 6), the temperature drops down and the temperature difference between the wall and free surface increases. So, the temperature profile of the thin film swiftly decreases from the wall surface to the free surface. Figure 10 explores the behavior of Pr on the temperature profile $\theta(\eta)$. The graph shows that with the increasing values of Pr = 0.1, 0.5, 1, 5, the temperature decreases. A higher Pr implying lower thermal diffusivity is the main reason for the lowering in temperature distribution. Figure 11 portrays the effect of S on $f'(\eta)$ (velocity) that shows an increasing pattern. A higher unsteadiness parameter will increase the height of the thin film thickness, and it will allow the fluid to move more quickly.

5. Concluding Remarks

Heat transfer of hybrid nanofluid comprising graphene oxide plus silver/kerosene oil in a finite thin film on a stretching surface with variable thermal conductivity is inspected. The conducting PDEs are reduced into a couple of ODEs (nonlinear) through similarity transformation. The MATLAB bvp4c technique is used to gain its numerical solutions. Some important results obtained are as follows:

(i) The Nusselt number, temperature, and velocity fields are highly affected by the power-law index. Temperature and velocity fields are inversely proportional to the power-law index.

(ii) Solid volume fractions of hybrid nanofluid impose great effects on the local Nusselt number, velocity, and temperature profiles.

(iii) The velocity of hybrid nanofluid decreases while the temperature increases with the increase in the value of solid volume fraction.

This article can further be enhanced by adding more prominent and valuable impacts such as thermal radiations and Joule heating. A magnetic field across the thin film can also be employed. Entropy analysis can also be done.

Nomenclature

Symbols

u, v: Velocity component along x and y directions
n: The power-law index
T: Fluid temperature
t: Time
C_p: Specific heat
k: The effective thermal conductivity of nanofluid
u_w: Sheet velocity
T_0: Temperature at the origin
T_{ref}: Reference temperature
T_w: Surface temperature of the nanofluid film
S: Unsteadiness parameter
h: Film thickness
Pr: Modified Prandtl number
Re_x: Local Reynolds number
Ec: Eckert number
nf: For the nanofluid
hnf: For the hybrid nanofluid
f: For the base fluid
s: For the solid (nanoparticles)
ϕ: Solid volume fraction
ρ: Density
ρ_{nf}: Effective density of nanofluid
$(\rho C_p)_{nf}$: Heat capacity of nanofluid
μ_{nf}: Viscosity coefficient of nanofluid
μ_f: Viscosity coefficient of base fluid
γ_f: Diffusivity of the nanofluid
α_{nf}: Thermal diffusivity of nanofluid
k_{nf}: Thermal conductivity of nanofluid
τ_{xy}: Shear stress
ψ: Stream function
η: Similarity variable
θ: Dimensionless temperature
β: Dimensionless film thickness.

Data Availability

No new data were created in this study.

Conflicts of Interest

The authors declare that they have no conflicts of interests.

Authors' Contributions

Ammar Alsinai conceptualized the study; Yasir Mehmood designed the methodology; Read S. A. Qahtan was responsible for software; Muhammad Bilal was responsible for formal analysis; Allah YarKhan, Read S. A. Qahtan, and Ammar Alsiani were responsible for the investigation of the study; Ammar Alsiani was responsible for the resources; Allah YarKhan, Ammar Alsinai, and Ramsha Shafqat wrote the original draft; Read S. A. Qahtan was responsible for reviewing and editing; Allah YarKhan and Ammar Alsiani supervised the study; Ammar Alsinai was responsible for project administration; Read S. A. Qahtan was responsible for funding acquisition.

References

[1] T. Gul, S. Islam, R. A. Shah, I. Khan, and S. Shafie, "Thin film flow in MHD third grade fluid on a vertical belt with temperature dependent viscosity," *PLoS One*, vol. 9, no. 6, Article ID e97552, 2014.

[2] M. R. Bachicha, "A Pseudo-plastic flow model for slurry deposition of thin film cathodes," Technical report, Sandia National Lab.(SNL-NM), Albuquerque, NM, USA, 2016.

[3] M. M. Aqil, M. A. Azam, M. F. Aziz, and R. Latif, "Deposition and characterization of molybdenum thin film using direct current magnetron and atomic force microscopy," *Journal of Nanotechnology*, vol. 2017, Article ID 4862087, 10 pages, 2017.

[4] Z. Shah, E. Bonyah, S. Islam, W. Khan, and M. Ishaq, "Radiative MHD thin film flow of Williamson fluid over an unsteady permeable stretching sheet," *Heliyon*, vol. 4, no. 10, Article ID e00825, 2018.

[5] S. Ullah, K. Akhtar, N. Khan, and A. Ullah, "Analysis of thin film flow of generalized Maxwell fluid confronting withdrawal and drainage on non-isothermal cylindrical surfaces,"

Advances in Mechanical Engineering, vol. 11, no. 10, Article ID 168781401988100, 2019.

[6] A. J. Chamkha and C. Issa, "Effects of heat generation/absorption and thermophoresis on hydromagnetic flow with heat and mass transfer over a flat surface," *International Journal of Numerical Methods for Heat and Fluid Flow*, vol. 10, no. 4, pp. 432–449, 2000.

[7] M. G. Reddy, "Heat generation and thermal radiation effects over a stretching sheet in a micropolar fluid," *ISRN Thermodynamics*, vol. 2012, Article ID 795814, 6 pages, 2012.

[8] Y. Mehmood, R. Shafqat, I. E. Sarris, M. Bilal, T. Sajid, and T. Akhtar, "Numerical investigation of mwcnt and swcnt fluid flow along with the activation energy effects over quartic auto catalytic endothermic and exothermic chemical reactions," *Mathematics*, vol. 10, no. 24, p. 4636, 2022.

[9] G. M. Pavithra and B. J. Gireesha, "Effect of internal heat generation/absorption on dusty fluid flow over an exponentially stretching sheet with viscous dissipation," *Journal of Mathematics*, vol. 2013, Article ID 583615, 10 pages, 2013.

[10] N. Yeşiller, J. L. Hanson, and E. H. Yee, "Waste heat generation: a comprehensive review," *Waste Management*, vol. 42, pp. 166–179, 2015.

[11] B. Ganga, S. Saranya, N. Vishnu Ganesh, and A. K. Abdul Hakeem, "Effects of space and temperature dependent internal heat generation/absorption on MHD flow of a nanofluid over a stretching sheet," *Journal of Hydrodynamics*, vol. 27, no. 6, pp. 945–954, 2015.

[12] M. Awais, T. Hayat, S. Irum, and A. Alsaedi, "Heat generation/absorption effects in a boundary layer stretched flow of Maxwell nanofluid: analytic and numeric solutions," *PLoS One*, vol. 10, no. 6, Article ID e0129814, 2015.

[13] A. Aziz, A. Alsaedi, T. Muhammad, and T. Hayat, "Numerical study for heat generation/absorption in flow of nanofluid by a rotating disk," *Results in Physics*, vol. 8, pp. 785–792, 2018.

[14] F. Mabood, G. Bognár, and A. Shafiq, "Impact of heat generation/absorption of magnetohydrodynamics Oldroyd-B fluid impinging on an inclined stretching sheet with radiation," *Scientific Reports*, vol. 10, no. 1, pp. 17688–17712, 2020.

[15] W. A. Khan, H. Sun, M. Shahzad, M. Ali, F. Sultan, and M. Irfan, "Importance of heat generation in chemically reactive flow subjected to convectively heated surface," *Indian Journal of Physics*, vol. 95, no. 1, pp. 89–97, 2021.

[16] K. V. Wong and O. De Leon, "Applications of nanofluids: current and future," *Advances in Mechanical Engineering*, vol. 2, Article ID 519659, 2010.

[17] C. Kleinstreuer and Y. Feng, "Experimental and theoretical studies of nanofluid thermal conductivity enhancement: a review," *Nanoscale Research Letters*, vol. 6, no. 1, pp. 229–313, 2011.

[18] D. Madhesh and S. Kalaiselvam, "Experimental analysis of hybrid nanofluid as a coolant," *Procedia Engineering*, vol. 97, pp. 1667–1675, 2014.

[19] T. Hayat and S. Nadeem, "Heat transfer enhancement with Ag–CuO/water hybrid nanofluidAg--CuO/water hybrid nanofluid," *Results in Physics*, vol. 7, pp. 2317–2324, 2017.

[20] L. S. Sundar, K. V. Sharma, M. K. Singh, and A. C. M. Sousa, "Hybrid nanofluids preparation, thermal properties, heat transfer and friction factor: a review," *Renewable and Sustainable Energy Reviews*, vol. 68, pp. 185–198, 2017.

[21] A. A. Minea and M. G. Moldoveanu, "Overview of hybrid nanofluids development and benefits," *Journal of Engineering and Thermophysics*, vol. 27, no. 4, pp. 507–514, 2018.

[22] S. Dinarvand, M. N. Rostami, and I. Pop, "A novel hybridity model for TiO2-CuO/water hybrid nanofluid flow over a static/moving wedge or corner," *Scientific Reports*, vol. 9, no. 1, pp. 1–11, 2019.

[23] R. K. Bumataria, N. K. Chavda, and H. Panchal, "Current research aspects in mono and hybrid nanofluid based heat pipe technologies," *Heliyon*, vol. 5, no. 5, Article ID e01627, 2019.

[24] M. Bilal, I. Asghar, M. Ramzan et al., "Dissipated electroosmotic EMHD hybrid nanofluid flow through the microchannel," *Scientific Reports*, vol. 12, no. 1, p. 4771, 2022.

[25] M. Bilal, I. Siddique, A. Borawski, A. Raza, M. Nadeem, and M. Sallah, "Williamson magneto nanofluid flow over partially slip and convective cylinder with thermal radiation and variable conductivity," *Scientific Reports*, vol. 12, no. 1, Article ID 12727, 2022.

[26] M. Bilal, M. Ramzan, I. Siddique, and A. Anum, "A numerical simulation of electrically conducting micro-channel nanofluid flow with thermal slip effects," *Waves in Random and Complex Media*, vol. 2022, pp. 1–25, 2022.

[27] M. Massoudi and I. Christie, "Effects of variable viscosity and viscous dissipation on the flow of a third grade fluid in a pipe," *International Journal of Non-linear Mechanics*, vol. 30, no. 5, pp. 687–699, 1995.

[28] Z. Mehmood, Z. Iqbal, E. Azhar, and E. N. Maraj, "Nanofluidic transport over a curved surface with viscous dissipation and convective mass flux," *Zeitschrift für Naturforschung A*, vol. 72, no. 3, pp. 223–229, 2017.

[29] A. K. Pandey and M. Kumar, "Effect of viscous dissipation and suction/injection on MHD nanofluid flow over a wedge with porous medium and slip," *Alexandria Engineering Journal*, vol. 55, no. 4, pp. 3115–3123, 2016.

[30] N. Ahmed, U. Khan, and S. T. Mohyud-Din, "Influence of viscous dissipation on a copper oxide nanofluid in an oblique channel: implementation of the KKL model," *The European Physical Journal Plus*, vol. 132, no. 5, pp. 1–12, 2017.

[31] A. Mishra and M. Kumar, "Influence of viscous dissipation and heat generation/absorption on Ag-water nanofluid flow over a Riga plate with suction," *International Journal of Fluid Mechanics Research*, vol. 46, no. 2, pp. 113–125, 2019.

[32] D. Saxena, "Study of viscous dissipation and convection of heat transfer over a flat plate with variable temperature using homotopy perturbation technique," in *Proceedings of International Conference on Advancements in Computing & Management (ICACM)*, Amsterdam, Netherlands, July 2019.

[33] S. Masood, M. Farooq, and S. Ahmad, "Description of viscous dissipation in magnetohydrodynamic flow of nanofluid: applications of biomedical treatment," *Advances in Mechanical Engineering*, vol. 12, no. 6, Article ID 168781402092635, 2020.

[34] M. Guedda and R. Kersner, "Non-Newtonian pseudoplastic fluids: analytical results and exact solutions," *International Journal of Non-linear Mechanics*, vol. 46, no. 7, pp. 949–957, 2011.

[35] K. Ma, S. Yuan, H. Chang, and H. Lai, "Experimental study of pseudoplastic fluid flows in a square duct of strong curvature," *Journal of Thermal Science*, vol. 23, no. 4, pp. 359–367, 2014.

[36] S. Das, A. S. Banu, R. N. Jana, and O. D. Makinde, "Entropy analysis on MHD pseudo-plastic nanofluid flow through a vertical porous channel with convective heating," *Alexandria Engineering Journal*, vol. 54, no. 3, pp. 325–337, 2015.

[37] K. Ayoubi Ayoubloo, M. Ghalambaz, T. Armaghani, A. Noghrehabadi, and A. J. Chamkha, "Pseudoplastic natural convection flow and heat transfer in a cylindrical vertical cavity partially filled with a porous layer," *International Journal of Numerical Methods for Heat and Fluid Flow*, vol. 30, no. 3, pp. 1096–1114, 2019.

[38] Y. Lin, L. Zheng, and G. Chen, "Unsteady flow and heat transfer of pseudo-plastic nanoliquid in a finite thin film on a stretching surface with variable thermal conductivity and viscous dissipation," *Powder Technology*, vol. 274, pp. 324–332, 2015.

[39] M. Bilal, M. Ramzan, R. Zafar, and I. Siddique, "A finite thin film flow of pseudo-plastic MHD hybrid nanofluid with heat generation and variable thermal conductivity," *Waves in Random and Complex Media*, vol. 2023, pp. 1–23, 2023.

[40] C. Wang and I. Pop, "Analysis of the flow of a power-law fluid film on an unsteady stretching surface by means of homotopy analysis method," *Journal of Non-newtonian Fluid Mechanics*, vol. 138, no. 2-3, pp. 161–172, 2006.